KV Cache is 1 Bit Per Channel: Efficient Large Language Model Inference with Coupled Quantization

Tianyi Zhang
Dept. of Computer Science, Rice University
xMAD.ai
Houston, TX
tz21@rice.edu

Jonah Yi
Dept. of Computer Science, Rice University
xMAD.ai
Houston, TX
jwy4@rice.edu

Zhaozhuo Xu
Dept. of Computer Science,
Stevens Institute of Technology
xMAD.ai
Hoboken, NJ
zxu79@stevens.edu

Anshumali Shrivastava
Dept. of Computer Science, Rice University
Ken Kennedy Institute
ThirdAI Corp.
xMAD.ai
Houston, TX
anshumali@rice.edu

Abstract

Efficient deployment of Large Language Models (LLMs) requires batching multiple requests together to improve throughput. As batch size, context length, or model size increases, the size of key and value (KV) cache quickly becomes the main contributor to GPU memory usage and the bottleneck of inference latency and throughput. Quantization has emerged as an effective technique for KV cache compression, but existing methods still fail at very low bit widths. Currently, KV cache quantization is performed per-channel or per-token independently. Our analysis shows that distinct channels of a key/value activation embedding are highly interdependent, and the joint entropy of multiple channels grows at a slower rate than the sum of their marginal entropy, which implies that per-channel independent quantization is sub-optimal. To mitigate this sub-optimality, we propose Coupled Quantization (CQ), which couples multiple key/value channels together for quantization to exploit their interdependence and encode the activations in a more information-efficient manner. Extensive experiments reveal that CQ compares favorably with existing baselines in preserving model quality, and improves inference throughput by 1.4–3.5$\times$ relative to the uncompressed baseline. Furthermore, we demonstrate that CQ can preserve model quality reasonably with KV cache quantized down to 1 bit.

1 Introduction

Large Language Models (LLMs) have showcased remarkable generalization abilities across various tasks without needing specific fine-tuning [30]. These impressive capabilities have empowered LLMs to find applications in numerous domains [19]. However, the high computational demands and prohibitive deployment costs of LLMs create significant barriers, hindering their widespread adoption [19, 4]. Particularly, as LLMs move towards larger model size [14] and longer context length [40], they require faster hardware accelerators such as graphics processing units (GPUs) with higher memory capacity for efficient inference. Hence it is crucial to develop approaches for reducing the computational costs and memory requirement of LLMs.

38th Conference on Neural Information Processing Systems (NeurIPS 2024).

Key and value (KV) caching [47] has proven to be an effective technique for accelerating LLM inference without affecting model quality. In autoregressive LLMs, KV caching works through trading off memory to save computations: the key and value activations of all previous tokens in the current sequence are cached in memory to avoid their recomputation for generating the next token. However, KV cache can quickly overwhelm the memory capacity of GPUs as context length or batch size increases, since its storage scales linearly with these two factors. Consider the OPT-175b model [43], storing its KV cache for 128 sequences of 2048 tokens requires 1.2 terabytes of memory, which is around 3.5× the storage of its weights. Because inference throughput scales with batch size, the substantial memory demands of KV caching can become a significant bottleneck to throughput. In addition, as KV cache is not shared across sequences within a batch, it has a low compute-to-memory ratio, making reading the KV cache from GPU memory the primary source of latency as opposed to the attention computation [15]. KV cache compression can bring the following benefits: 1. speeding up LLM inference by improving the compute-to-memory ratio, 2. improving the serving throughput by fitting more sequences into memory and hence enabling larger batch sizes, 3. lowering the GPU requirements for inference for a given batch size, context length, and model size. Existing approaches typically achieve compression of KV cache through token eviction [47, 24] or activation quantization [25, 15]. While these methods can preserve model quality at moderate compression rates (4× compression or 4 bits per activation), model quality quickly deteriorates at high compression rates (16× compression or 1 bit per activation). In this work, we leverage the interdependency between key/value channels, an insight overlooked by existing approaches, to achieve higher compression rates of KV cache while maintaining model quality.

Our approach is motivated by the observation that distinct channels within the same key/value activation embedding are highly interdependent and correlated (see our analysis in Section 3.1). It is hence more information-efficient to encode multiple channels of KV cache at once, which we call *channel coupling*. Existing solutions, in contrast, only employ per-channel or per-token quantization strategies [25, 15] for compressing KV cache, which is not optimal for exploiting the dependency between channels. As a result, we observe significant model quality degradation at the extreme compression rate of 1 bit per activation. By leveraging channel coupling, we enable compression at the level of 1-bit quantization of KV cache while preserving model quality. In Figure 1, we show the perplexity of two models from the LLaMA family [36, 37] on WikiText-2 [27] under 1-bit quantization with varying numbers of coupled channels. The full experimental setup is presented in Section 4. Coupling more channels significantly enhances model quality, as the perplexity quickly approaches the performance using uncompressed FP16 KV cache. By further combining KV cache quantization with a sliding window of 128 recent tokens cached in full precision, we achieve a negligible 0.3–0.33 increase in perplexity with 1-bit KV cache.

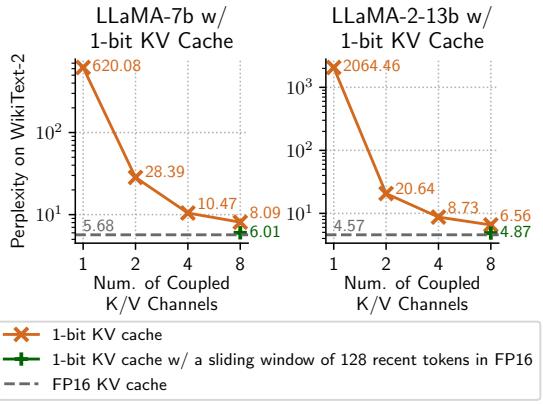

Figure 1: Perplexity of LLMs with 1-bit quantized KV cache approaches the uncompressed FP16 performance as the number of coupled K/V channels increases.

We summarize our contributions as follows.

1. We observe the phenomenon that distinct channels within the same key/value activation embedding share a high amount of dependency or mutual information, which has not been leveraged by existing approaches.
2. We propose Coupled Quantization (CQ), a novel KV cache quantization method that jointly encodes multiple key/value channels to exploit the dependency across channels.
3. Through extensive experiments, we demonstrate the effectiveness of CQ at preserving model quality and speeding up LLM inference against competitive baselines. Furthermore, we demonstrate CQ reasonably preserves model quality at an extreme level of 1-bit quantization.

2 Background

This section introduces the relevant background information including the KV caching technique and per-channel quantization.

2.1 LLM Attention and KV Cache

Decoder-only transformer-based LLMs employ masked self-attention [38], in which activations of the current token only depend on the previous tokens and are unaffected by future ones. This property enables training parallelism for the next-token prediction objective, and gives rise to the KV caching technique for efficient decoding during inference. Consider the decoding step for the t-th token in a single head of attention in an LLM. The input embedding of the t-th token (a column vector), e_t, goes through three distinct transformations to become key, query, and value activation embeddings $f_K(e_t), f_Q(e_t), f_V(e_t)$, where the transformations f_K, f_Q, f_V are composed of linear projection and positional encoding methods such as RoPE [35]. The output embedding of attention for the t-th token is computed as

$$\text{attention}(e_t) = \begin{bmatrix} f_V(e_1) & \dots & f_V(e_t) \end{bmatrix} \text{softmax}\left(\begin{bmatrix} f_K(e_1) & \dots & f_K(e_t) \end{bmatrix}^\top f_Q(e_t) \Big/ \sqrt{d} \right) \quad (1)$$

where d is the dimensionality of $f_K(e_t)$. Computing the output embedding of the current token requires the key and value activation embeddings of all previous tokens, $f_K(e_i)$ and $f_V(e_i)$ where $i \in \{1, \dots, t-1\}$. These embeddings are cached in memory from previous decoding steps to eliminate redundant computations, a process known as KV caching. The size of KV cache can be calculated as $b \times n \times l \times 2 \times h \times d$ floating-point numbers, where b is the batch size, n is the number of tokens in each sequence, l is the number of layers in the model, 2 is for key and value, h is the number of key/value attention heads, and d is the dimensionality of a single head of key/value activation embedding. As batch size, context length, or model size increases, the size of the KV cache can quickly overwhelm the limited GPU memory. KV cache bottlenecks inference throughput since it limits the maximum batch size, and it is a major contributor to latency due to the low compute-to-memory ratio [15].

2.2 Per-Channel Quantization

Existing KV cache quantization methods [15, 25] employ per-channel quantization for keys and per-token quantization for values. Per-channel and per-token quantization are similar, except the direction along which the quantization centroids are learned (or the direction along which the scaling factor and zero-point are determined for uniform quantization). Keys are quantized per-channel based on the observation that certain key channels have significantly higher magnitudes than others, while values are quantized per-token because value channels have no such outliers. In non-uniform per-channel quantization, a set of centroids is learned for each channel. Suppose A is a key or value activation matrix, and let $A_{i,:}$ denote the i-th channel of A. Then, non-uniform b-bit per-channel quantization aims to learn a set of centroids $C_i^\star \subset \mathbb{R}$ for each channel i of A through the objective

$$C_i^\star = \underset{\substack{C \subset \mathbb{R} \\ |C| = 2^b}}{\arg\min} \left\| A_{i,:} - q(A_{i,:}) \right\|_2^2 \quad (2)$$

where q quantizes each value in $A_{i,:}$ to the nearest centroid in C.

3 Methodology

In this section, we motivate our proposal using information theory and introduce the Coupled Quantization (CQ) approach for KV cache compression.

3.1 Motivations

Our proposed approach is inspired by concepts in information theory [33]. We consider channels in a key/value activation embedding as random variables $X_1, X_2, \dots$. The amount of information (or uncertainty) in channel X can be measured by *entropy*, defined as $H(X) = -\int_{\mathbb{X}} p(x) \log_2 p(x)\, dx$,

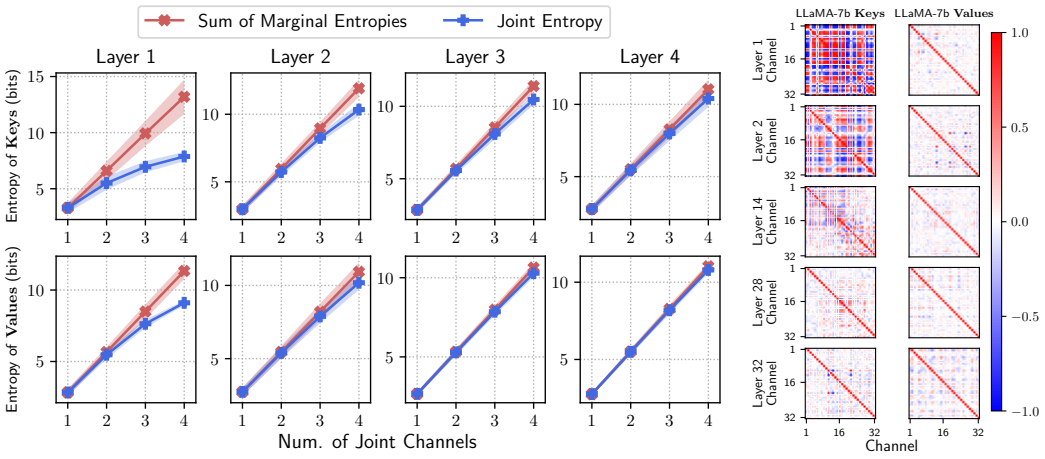

(a) (b)

Figure 2: (a) Growth rate of joint entropy versus sum of marginal entropies of the key/value activation embeddings of LLaMA-7b on 262k tokens of WikiText-2. Entropy is estimated using Equation 4. The slower growth rate of joint entropy implies that quantizing more channels together is more information-efficient than quantizing fewer channels. (b) Correlation matrices of the first 32 channels of 5 layers of LLaMA-7b key and value activation embeddings on WikiText-2. Channel pairs exhibit high levels of linear dependency, shown by high magnitudes of the correlation coefficients.

where $p(\cdot)$ is the probability density function and $\mathbb{X}$ is the support of X. $H(X)$ measures the theoretical number of bits needed for losslessly encoding the channel X, hence it can be used to gauge how "quantizable" a channel is: if $H(X_1) < H(X_2)$, then channel X_1 may be quantized to fewer bits than channel X_2 with the same quantization error.

Our insight is that different channels from the same key/value activation embedding may be interdependent, which would reduce the number of bits required for jointly encoding multiple channels together compared to encoding them independently. The total amount of information (or uncertainty) in two channels X_1, X_2 is measured by *joint entropy*, defined as $H(X_1, X_2) = -\int_{\mathbb{X}_1}\int_{\mathbb{X}_2} p(x_1, x_2)\log_2 p(x_1, x_2)\,dx_2\,dx_1$, where $p(\cdot,\cdot)$ is the joint probability density function. Equivalently, the joint entropy of two channels is the difference between the sum of their marginal entropies and their mutual information, i.e., $H(X_1, X_2) = H(X_1) + H(X_2) - I(X_1, X_2)$, where $I(\cdot,\cdot)$ is a non-negative quantity for measuring the mutual dependency of two random variables. Thus, we have

$$H(X_1, X_2) \leq H(X_1) + H(X_2) \tag{3}$$

which implies the number of bits needed for jointly encoding two channels is no more than the total number of bits needed for encoding them independently. Previous works have demonstrated that deep neural networks [16] and attention-based networks [9] tend to produce low-rank embeddings, which suggests that channels of key/value embedding in LLM may exhibit high amount of mutual dependency.

It is hence beneficial to measure the difference between the sum of marginal entropies of multiple key/value channels and their joint entropy. A significant difference would suggest that encoding these channels together is more information-efficient than encoding them independently. However, it is difficult to derive the exact entropy or joint entropy of channels, since their probability density functions are not known. Therefore, we employ the "binning" trick [21] to estimate entropy. We first observe an empirical distribution of key and value channels by saving the KV cache on a dataset, and partition the support of each channel into equally sized bins. Then, values of each channel are discretized to the index of the bin they fall into. Finally, the joint entropy of n channels $X_1, \ldots, X_n$ is estimated with the Riemann sum,

$$H(X_1, \ldots, X_n) \approx \sum_{x_1 \in \mathbb{B}_1} \cdots \sum_{x_n \in \mathbb{B}_n} \hat{p}(x_1, \ldots, x_n)\log_2 \hat{p}(x_1, \ldots, x_n) \tag{4}$$

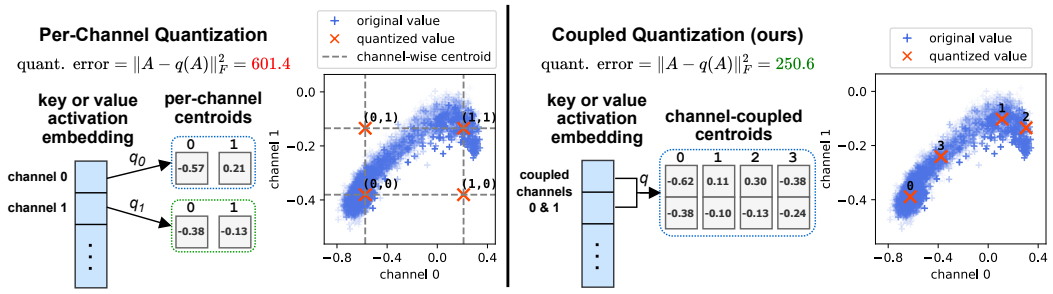

Figure 3: Per-channel quantization (left) and our proposed Coupled Quantization (right). The 1-bit quantization results on the first two channels of the first-layer key activation embeddings of LLaMA-7b on the WikiText-2 dataset are shown. CQ leverages the dependency between channels to achieve lower quantization errors than per-channel quantization.

where $\mathbb{B}_i$ is the support of the binned or discretized X_i and $\hat{p}(\cdot)$ is the empirical probability mass function. Specifically, we divide the channels of key and value embeddings of LLaMA-7b [36] into non-overlapping groups each containing c contiguous channels, where $c \in \{1, 2, 3, 4\}$, and estimate the joint entropy and the sum of marginal entropies of each group. The support of each channel is partitioned into 16 equally sized bins. Figure 2a shows the mean and standard deviation of the estimated joint entropy and sum of marginal entropies of four layers of LLaMA-7b on 262k tokens of the WikiText-2 dataset [27], averaged over groups. We only show a maximum group size of 4, since increasing the group size requires saving exponentially more key and value embeddings to avoid empty bins and maintain estimation quality. As shown in Figure 2a, the sum of marginal entropies grows at a linear rate while the joint entropy increases slower at a sub-linear rate. This implies that as the number of jointly quantized channels increases, the total amount of information needed for encoding them decreases. This phenomenon is the foundation that motivates our proposed approach.

In addition to studying the marginal and joint entropy, we also analyze the linear relationships between channels of a key/value activation embedding using Pearson correlation coefficient. Figure 2b presents the correlation matrices for the first 32 channels of 5 layers of LLaMA-7b keys and values on WikiText-2. The key and value channels exhibit high levels of linear dependency, and are clearly not independently distributed, as shown by high magnitudes of the correlation coefficients. In Section M of the appendix, we include the correlation matrices of all layers of LLaMA-7b, and present scatter plots to visualize the patterns in key and value activations.

3.2 Coupled Quantization

Motivated by the finding that distinct key/value channels exhibit high amounts of dependency, we propose Coupled Quantization (CQ), an information-efficient KV cache quantization approach that couples multiple key/value channels for quantization. More concretely, channels of a key or value activation embedding are divided into equally sized, non-overlapping groups of contiguous channels. The channels in each group are *coupled*, as they are jointly quantized and share a single quantization code. For each group of coupled channels, a distinct set of multi-channel centroids are learned, where each centroid has dimensionality equal to the number of channels in that group. When quantizing a key or value activation embedding, each channel group is quantized to the nearest centroid in terms of L2 distance. We use the CQ-<c>c<b>b notation to denote the configuration of channel coupling and quantization bit width, where <c> is the number of channels in each group and <b> indicates the number of bits in a quantized code for a group. For example, CQ-4c8b means that every 4 contiguous channels are coupled together and each coupled group shares an 8-bit code, which is equivalent to 2-bit per-channel quantization in terms of storage overhead of quantized codes. An illustrative comparison of per-channel quantization and CQ is shown in Figure 3. Although previous works [15, 25] opt to quantize keys per-channel and values per-token, we adopt channel-coupled quantization for both keys and values, which we empirically show is effective for both in Section 4.3. CQ quantizes keys before the positional encoding such as RoPE [35] is applied, which increases the quantization difficulty by introducing more outliers in key activations [15, 25].

3.2.1 Centroid Learning

In CQ, the multi-channel centroids for each channel group are learned offline on a calibration dataset by leveraging uniform clustering or second-order-information-informed clustering. Specifically, for uniform centroid learning of the CQ-ccbb configuration, a set of centroids $C_i^\star \subset \mathbb{R}^c$ is learned independently for each channel group i through the objective

$$C_i^\star = \underset{\substack{C\subset\mathbb{R}^c \\ |C|=2^b}}{\arg\min} \left\| A_{(ic-c+1):ic,:} - \mathrm{cq}\left(A_{(ic-c+1):ic,:}\right) \right\|_F^2 \tag{5}$$

where $A_{(ic-c+1):ic,:}$ is the sub-matrix of A containing all coupled channels from the i-th group, and cq quantizes each column vector to the nearest centroid in C in terms of L2 distance. We use the k-means algorithm [26] with k-means++ initialization [1] to optimize the objective.

LLMs are more sensitive to the quantized precision of certain weights than others [20], hence centroids of CQ should be learned to bias towards preserving the precision of more important activations. To this end, we leverage an approximation to the Hessian to perform second-order-information-informed centroid learning. More concretely, we use the diagonals of the Fisher information matrix $\mathcal{F}$ to identify the more influential key/value activations and guide the centroid learning process. Using the diagonal Fisher information matrix for quantization was proposed in [22], and we extend it to the multi-channel case. For performing Fisher-guided centroid learning, we first save a key/value activation matrix A and its gradient $g(A) = \frac{\partial}{\partial A}\mathcal{L}(A)$ on a calibration dataset, where $\mathcal{L}$ is the training loss function. We approximate the Hessian matrix using the diagonals of the Fisher information matrix, $\mathrm{diag}(\mathcal{F}) = g(A) \odot g(A)$, which is the element-wise square of the gradient matrix. We use the sum of diagonal entries of the Fisher information matrix as a measure of importance for each group of activations, and obtain the centroid set $C_i^\star$ for the i-th channel group using the objective

$$C_i^\star = \underset{\substack{C\subset\mathbb{R}^c \\ |C|=2^b}}{\arg\min} \sum_j \underbrace{g\left(A_{(ic-c+1):ic,\,j}\right)^\top g\left(A_{(ic-c+1):ic,\,j}\right)}_{\text{partial sum of } \mathrm{diag}(\mathcal{F})} \left\| A_{(ic-c+1):ic,\,j} - \mathrm{cq}(A_{(ic-c+1):ic,\,j}) \right\|_2^2 \tag{6}$$

which we leverage weighted k-means to optimize. We discuss the overhead of centroid learning and centroid storage in Section E in the appendix.

3.3 Efficient Inference Through Kernel Fusion

We design fused GPU kernels to enable efficient inference of CQ. During inference, dequantizing couple-quantized KV cache requires many random accesses for lookups of multi-dimensional centroids. If the centroids reside in GPU global memory, these random accesses would greatly hinder the inference efficiency. We circumvent this issue by caching centroids in the shared memory, which has significantly lower latency and higher bandwidth than global memory. Due to limited size of the shared memory for each thread block, we assign the work of a single channel group to each thread block, which only requires loading a single group of centroids into a block of shared memory. We perform kernel fusion to merge dequantization of key cache, positional encoding and KQ multiplication, as well as to merge dequantization of value cache and its multiplication with attention scores. We validate the inference efficiency of CQ empirically in Section 4.4.

4 Experiments

In this section, we perform extensive experiments to validate the effectiveness of our proposed CQ approach for KV cache compression. We first introduce the experimental setups including hardware, software, datasets, metrics, and baselines used. Then, we present the detailed empirical results and provide discussions. Finally, we perform an ablation study to validate the effectiveness of each component of our proposal.

Hardware and Software Experiments are performed on a Linux server equipped with 4 NVIDIA A100 40GB GPUs. Our software implementation of CQ is based on PyTorch [29] and the HuggingFace Transformers library [39].

Evaluation Metrics and Datasets We compare different KV cache quantization by evaluating the quality of 5 LLMs on various benchmarks. The 5 LLMs considered are 1. LLaMA-7b, 2. LLaMA-13b

Table 1: Perplexity of LLMs on WikiText-2 under different KV cache quantization methods at varying bit widths. The results of INT, NF, and KVQuant (except -1b and -1b+1% sparse) are from [15]. "NaN" means Not a Number, which is caused by quantization numerical instability. Our proposed method CQ outperforms baselines under the same bit width.

	Bits Per Activation	LLaMA-7b	LLaMA-13b	LLaMA-2-7b	LLaMA-2-13b	Mistral-7b
FP16	16	5.68	5.09	5.12	4.57	4.76
INT4	4.00	5.98	5.32	5.66	5.01	4.97
INT4-g128	4.16	5.77	5.16	5.32	4.71	4.82
NF4	4.00	5.87	5.23	5.47	4.90	4.91
NF4-g128	4.25	5.77	5.17	5.30	4.71	4.83
KVQuant-4b	4.00	5.73	5.15	5.18	4.63	4.81
KVQuant-4b+1% sparse	4.32	**5.70**	**5.11**	**5.14**	**4.59**	**4.78**
CQ-2c8b	4.00	**5.70**	**5.11**	**5.14**	**4.59**	4.79
INT2	2.00	11779	69965	4708	3942	573
INT2-g128	2.14	37.37	41.77	117.88	93.09	51.96
NF2	2.00	3210.5	5785.6	13601	4035.6	902.51
NF2-g128	2.25	351.23	141.19	634.59	642.44	252.85
KVQuant-2b	2.00	8.17	7.29	9.75	29.25	7.33
KVQuant-2b+1% sparse	2.32	6.06	5.40	5.50	4.92	5.16
CQ-4c8b	2.00	5.97	5.32	5.42	4.81	5.11
CQ-4c9b	2.26	**5.88**	**5.26**	**5.32**	**4.74**	**4.98**
KVQuant-1b	1.00	321.58	1617.40	NaN	4709.83	203.73
KVQuant-1b+1% sparse	1.32	9.93	7.97	9.50	13.76	10.07
CQ-8c8b	1.00	8.09	7.02	7.75	6.55	7.25
CQ-8c10b	1.27	**6.78**	**6.00**	**6.25**	**5.47**	**5.90**

[36], 3. LLaMA-2-7b, 4. LLaMA-2-13b [37], 5. Mistral-7b [18]. We evaluate the quality of LLMs using the metric perplexity on 2 datasets: WikiText-2 [27] and C4 [31], and zero-shot accuracy on 3 benchmarks: WinoGrande [32], PIQA [3], and ARC Challenge (Arc-C) [5]. Furthermore, we evaluate on long-context benchmarks GSM8K [6] with chain-of-thought (CoT), and few-shot MMLU [13] with CoT. For perplexity and accuracy evaluations, the KV cache of all tokens in all layers is quantized, during both the prefill and decoding stages. The experimental details, including the procedures for perplexity and benchmark evaluations, are presented in Section A in the Appendix. More experimental results, including a comparison between CQ and KIVI [25] on LongBench [2], and results on more models and passkey retrieval [28], can be found in the Appendix.

Baselines We compare our proposed approach with uncompressed FP16 KV cache and competitive KV cache quantization methods, including 1. uniform integer (INT) quantization (without grouping and with a group size of 128), 2. NormalFloat (NF) quantization [8] (without grouping and with a group size of 128), 3. KVQuant [15] (dense-only and with 1% outliers stored in sparse format). KVQuant-<b>b+1% sparse is a dense-and-sparse method that stores outlier activations in a sparse matrix and requires an additional sparse matrix multiplication during inference, which introduces extra computational overhead. For calibration, we use the same set of 16 sequences of WikiText-2, each with 2048 tokens, for KVQuant and CQ. Other methods do not require calibration. Calibration is performed only once and the learned centroids are used for all downstream evaluations. Calibration is done on the training set of WikiText-2, while perplexity and accuracy are evaluated on the test sets of different datasets and benchmarks. For 1-bit and 2-bit KVQuant, we employ Q-Norm to mitigate distribution shift, as recommended by [15]. We report Bits Per Activation (BPA) to measure the compression rate of each method, where each activation in the uncompressed KV cache is a 16-bit float. Detailed calculations of bits per activation for CQ are presented in Section F in the appendix.

4.1 Results

Table 1 presents the perplexity of LLMs on WikiText-2 under different KV quantization methods. CQ consistently outperforms baselines under the same quantization bit width. In low bit width regions of 1-bit and 2-bit quantization, dense-only quantization baselines quickly deteriorates in quality while CQ preserves quality well. We highlight that CQ-8c8b (1 bit per activation) outperforms KVQuant-2b (2 bits per activation) with only half the memory. CQ also compares favorably against

Table 2: Accuracy of LLMs on 3 benchmarks under different KV cache quantization methods at varying bit widths.

	Bits Per Activation	Benchmark	LLaMA-7b	LLaMA-13b	LLaMA-2-7b	LLaMA-2-13b	Mistral-7b	Average
FP16	16	WinoGrande	69.93	72.69	68.90	71.98	73.88	65.55
		PIQA	78.67	79.16	78.07	79.16	80.58	
		ARC-C	41.72	46.42	43.43	48.29	50.34	
KVQuant-4b	4.00	WinoGrande	69.53	72.61	67.96	71.59	**73.88**	65.17
		PIQA	**78.62**	**79.22**	77.86	78.94	80.58	
		ARC-C	**42.32**	45.99	42.75	46.67	49.06	
KVQuant-4b+1% sparse	4.32	WinoGrande	**70.72**	**73.40**	**68.67**	72.30	73.72	65.57
		PIQA	78.40	79.16	**78.07**	**79.27**	**80.74**	
		ARC-C	41.38	**46.76**	43.17	**47.87**	**49.91**	
CQ-2c8b	4.00	WinoGrande	70.40	72.45	68.27	**72.53**	73.48	65.31
		PIQA	78.61	79.11	77.91	78.62	80.52	
		ARC-C	41.55	45.99	**43.34**	47.78	49.15	
KVQuant-2b+1% sparse	2.32	WinoGrande	68.03	**71.43**	**67.64**	70.17	**70.80**	63.79
		PIQA	**77.69**	**78.51**	76.60	**78.51**	**79.65**	
		ARC-C	38.74	**45.14**	41.47	**44.97**	47.53	
CQ-4c9b	2.26	WinoGrande	**68.51**	69.93	67.40	**71.67**	70.71	63.75
		PIQA	76.82	**78.51**	**77.09**	77.31	79.48	
		ARC-C	**39.16**	**45.14**	**41.64**	**44.97**	**47.95**	
KVQuant-2b	2.00	WinoGrande	53.59	59.35	51.70	51.30	63.46	52.20
		PIQA	72.47	74.81	63.38	65.40	75.46	
		ARC-C	32.00	34.47	22.44	24.66	38.57	
CQ-4c8b	2.00	WinoGrande	**67.48**	**70.72**	**66.45**	**69.06**	**69.38**	62.85
		PIQA	**76.11**	**78.29**	**76.12**	**77.42**	**79.49**	
		ARC-C	**38.48**	**44.03**	**39.93**	**44.11**	**45.65**	
KVQuant-1b+1% sparse	1.32	WinoGrande	56.67	61.01	57.77	57.30	58.17	54.31
		PIQA	71.38	75.46	69.91	70.89	73.83	
		ARC-C	29.69	35.32	31.48	32.59	33.19	
CQ-8c10b	1.27	WinoGrande	**60.46**	**65.27**	**59.19**	**62.98**	**63.93**	57.95
		PIQA	**73.45**	**75.90**	**73.07**	**74.37**	**77.31**	
		ARC-C	**33.28**	**37.12**	**34.64**	**38.74**	**39.59**	
KVQuant-1b	1.00	WinoGrande	50.51	48.46	50.91	49.41	49.80	41.35
		PIQA	53.26	53.54	53.37	50.92	54.73	
		ARC-C	21.76	21.33	20.65	21.67	19.88	
CQ-8c8b	1.00	WinoGrande	**56.51**	**61.56**	**55.01**	**57.14**	**58.25**	54.36
		PIQA	**71.16**	**73.99**	**71.22**	**73.01**	**75.24**	
		ARC-C	**30.20**	**33.79**	**30.20**	**34.30**	**33.79**	

Table 3: Accuracy of LLaMA-2-7b on 5 long-context benchmarks under different KV cache quantization methods at varying bit widths.

	Bits Per Activation	GSM8K, CoT	MMLU, CoT Fewshot			
			STEM	Humanities	Social	Other
FP16	16	13.57	33.43	41.12	50.74	56.60
KVQuant-4b+1% sparse	4.32	14.33	31.04	41.12	**48.37**	55.43
CQ-2c8b	4.00	**14.71**	**33.73**	**43.44**	47.77	**56.01**
KVQuant-2b+1% sparse	2.32	**10.31**	**28.06**	35.64	42.43	**46.39**
CQ-4c9b	2.26	**10.31**	27.76	**35.91**	**44.51**	45.75
KVQuant-2b	2.00	2.27	9.85	12.55	20.18	19.94
CQ-4c8b	2.00	**8.04**	**25.67**	**30.89**	**45.40**	**41.94**
KVQuant-1b+1% sparse	1.32	2.27	10.75	14.09	20.77	19.94
CQ-8c10b	1.27	**2.35**	**13.13**	**21.81**	**28.19**	**26.98**
KVQuant-1b	1.00	0.68	0.00	0.00	0.00	0.00
CQ-8c8b	1.00	**1.74**	**5.37**	**11.39**	**20.77**	**16.72**

dense-and-sparse baselines by outperforming KVQuant+1% sparse in most cases despite using less bits. We present the perplexity results on C4 in Table 7 in the appendix. Table 2 presents the accuracy results of KVQuant and CQ on different benchmarks. CQ consistently outperforms dense-only KVQuant at 1-bit and 2-bit, and performs better or on par with the dense-and-sparse KVQuant under the same bit width. Table 3 presents the accuracy comparison of KVQuant and CQ on long-context benchmarks, with CoT or few-shot CoT. CQ mostly outperforms KVQuant under similar bit widths.

Table 4: Accuracy of LLaMA-2 models with couple-quantized KV cache and a sliding window of 32 recent tokens cached in FP16. CQ achieves minimal accuracy degradation compared to the FP16 baseline.

	Quant.	BPA	WinoGrande	PIQA	Arc-C	Arc-E	Hellaswag	Average
LLaMA-2-7b	FP16	16	68.90	78.07	43.43	76.30	57.14	64.768
	CQ-2c8b	4.00	69.14	78.18	43.34	76.52	57.12	64.860 (+0.092)
	CQ-4c8b	2.00	69.06	77.86	42.83	76.01	56.79	64.510 (-0.258)
	CQ-8c8b	1.00	69.14	77.91	42.92	75.67	55.11	64.150 (-0.618)
LLaMA-2-13b	FP16	16	71.98	79.16	48.29	79.42	60.04	67.778
	CQ-2c8b	4.00	72.30	78.94	47.95	79.55	60.18	67.784 (+0.006)
	CQ-4c8b	2.00	72.30	78.89	47.61	79.21	59.84	67.570 (-0.208)
	CQ-8c8b	1.00	72.22	78.84	47.78	79.12	58.55	67.302 (-0.476)

4.2 Near-native Performance with Sliding Window Full-precision Cache

CQ mostly outperforms competitive baselines under the same bit width for fully quantized KV cache, and we further investigate the performance of CQ when combined with a sliding window of recent tokens cached in FP16 precision. This sliding window of full-precision cache only introduces a small constant memory overhead for each sequence. In Table 4, we present the accuracy of LLaMA-2 models on 5 benchmarks (WinoGrande, PIQA, Arc-C, Arc Easy (Arc-E) [5], and Hellaswag [42]) with a sliding window of 32 recent tokens in FP16 and the rest of the tokens coupled-quantized. CQ preserves the accuracy well, achieving a mere 0.476–0.618% loss in average accuracy over 5 tasks with 1-bit quantization. CQ also preserves perplexity well at 1-bit with a sliding window of 128 tokens in FP16, as shown in Figure 1.

Table 5: Ablative study on the effects of channel coupling for quantizing keys only, values only, and both keys and values, using 1-bit CQ. Perplexity of LLaMA-7b on WikiText-2 is reported.

	BPA	Perplexity ↓		
		Keys Only	Values Only	Keys & Values
CQ-1c1b	1.00	17.17	177.13	620.08
CQ-2c2b	1.00	8.29	9.49	28.39
CQ-4c4b	1.00	7.10	7.11	10.47
CQ-8c8b	1.00	6.53	6.54	8.09
FP16	16		5.68	

Table 6: Ablative study on the effects of Fisher-guided centroid learning for CQ. Perplexity of LLaMA-7b on WikiText-2 is reported.

	Centroids	Perplexity ↓
CQ-2c8b	Uniform	5.77
	Fisher-guided	5.70
CQ-4c8b	Uniform	6.86
	Fisher-guided	5.97
CQ-8c8b	Uniform	32.12
	Fisher-guided	8.09

4.3 Ablation Study

We perform a set of ablation experiments to answer the following questions. The experimental results are presented in Tables 5 & 6.

Q1: Under the same quantization bit width, does coupling more channels lead to better model quality? Yes, the model performance approaches the FP16 baseline level as the number of coupled channels increases, as shown in Table 5. This also holds true for different models and bit widths, as shown in Figure 1 and Table 8 in the appendix.

Q2: Is channel coupling effective for quantizing both keys and values? Yes, channel coupling is highly effective for both keys and values. As shown in Table 5, perplexity improves significantly under the same bit width as the number of coupled channels increases, and holds true for both key-only and value-only quantization.

Q3: Does Fisher-guided learning of centroids produce better model quality than uniform clustering? Yes, Fisher-guided centroid learning improves the model perplexity over uniform clustering, as shown in Table 6. Table 8 in the appendix further shows it is effective for different models.

4.4 Efficiency of CQ

We study the efficiency of CQ by comparing its decoding throughput with uncompressed FP16 KV cache using the HuggingFace Transformers implementation [39]. We measure the decoding throughput by running LLaMA-2-7b on an A100-40GB GPU with CQ and FP16 KV cache to process a 100-token prompt and generate 1000 tokens. We increase the inference batch size until the GPU runs out of memory. Results are presented in Figure 4. CQ achieves 3.75×, 7.5×, and 15× larger batch size than the FP16 baseline at 4-bit, 2-bit, 1-bit quantization, respectively. Moreover, CQ improves the decoding throughput by 1.4–3.5× relative to the FP16 baseline. Additional latency measurements for CQ are presented in Section K in the Appendix.

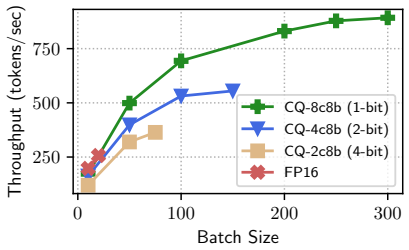

Figure 4: Inference throughput of CQ versus FP16 KV cache for LLaMA-2-7b.

5 Related Works

Existing works mitigate the high memory overhead of KV cache through token eviction, quantization, or tensor offloading. Scissorhands [24] and H2O [47] achieve KV cache compression while preserving model quality by storing only the pivotal tokens and evicting the unimportant ones. KIVI [25] proposes to quantize keys per-channel and values per-token using group-wise integer quantization. KVQuant [15] proposes sensitivity-based and dense-and-sparse quantization for KV cache to reduce quantization errors. Flexgen [34] proposes to offload KV cache instead of weights to enable high-throughput inference on a single GPU. Weight quantization [11, 23, 44] is an orthogonal line of work that reduce GPU memory requirements and improve effciency of LLM inference and fine-tuning [45]. FlashAttention [7] and NoMAD-Attention [46] are system optimizations for speeding up LLM inference on GPUs and CPUs, respectively. Product quantization [17] is a method for nearest neighbor search that compresses vectors by decomposing the vector space into a Cartesian product of low-dimensional subspaces, and quantizing each subspace independently.

6 Conclusion

We propose Coupled Quantization (CQ) for mitigating the latency and throughput bottleneck of LLM inference by quantizing KV cache. We discover that channels of KV cache are highly interdependent, which implies the existing approach of per-channel quantization approach is sub-optimal. We propose channel coupling to exploit the interdependency across channels to achieve more information-efficient encoding of key/value activations. Extensive experiments demonstrate that our method outperforms competitive baselines in model quality in most cases, and can reasonably preserve model quality with KV cache quantized down to 1 bit.

Acknowledgements

This work was supported by National Science Foundation SHF-2211815, Ken Kennedy Institute, and grants from Adobe and VMware.

Limitations & Broader Impacts

KV cache quantization is a form of lossy compression which inevitably affects model quality. Although we study its effects on perplexity and accuracy, it remains unclear how it affects other aspects of the model such as hallucination and adversarial robustness. Making LLM inference more efficient contributes to the democratization of artificial intelligence and the reduction of carbon footprints. We expect no additional negative societal impacts other than the ones already posed by LLMs.

References

[1] David Arthur, Sergei Vassilvitskii, et al. k-means++: The advantages of careful seeding. In *Soda*, volume 7, pages 1027–1035, 2007.

[2] Yushi Bai, Xin Lv, Jiajie Zhang, Hongchang Lyu, Jiankai Tang, Zhidian Huang, Zhengxiao Du, Xiao Liu, Aohan Zeng, Lei Hou, et al. Longbench: A bilingual, multitask benchmark for long context understanding. *arXiv preprint arXiv:2308.14508*, 2023.

[3] Yonatan Bisk, Rowan Zellers, Jianfeng Gao, Yejin Choi, et al. Piqa: Reasoning about physical commonsense in natural language. In *Proceedings of the AAAI conference on artificial intelligence*, volume 34, pages 7432–7439, 2020.

[4] Lingjiao Chen, Matei Zaharia, and James Zou. Frugalgpt: How to use large language models while reducing cost and improving performance. *arXiv preprint arXiv:2305.05176*, 2023.

[5] Peter Clark, Isaac Cowhey, Oren Etzioni, Tushar Khot, Ashish Sabharwal, Carissa Schoenick, and Oyvind Tafjord. Think you have solved question answering? try arc, the ai2 reasoning challenge. *arXiv preprint arXiv:1803.05457*, 2018.

[6] Karl Cobbe, Vineet Kosaraju, Mohammad Bavarian, Mark Chen, Heewoo Jun, Lukasz Kaiser, Matthias Plappert, Jerry Tworek, Jacob Hilton, Reiichiro Nakano, Christopher Hesse, and John Schulman. Training verifiers to solve math word problems. *arXiv preprint arXiv:2110.14168*, 2021.

[7] Tri Dao, Dan Fu, Stefano Ermon, Atri Rudra, and Christopher Ré. Flashattention: Fast and memory-efficient exact attention with io-awareness. *Advances in Neural Information Processing Systems*, 35:16344–16359, 2022.

[8] Tim Dettmers, Artidoro Pagnoni, Ari Holtzman, and Luke Zettlemoyer. Qlora: Efficient finetuning of quantized llms. *Advances in Neural Information Processing Systems*, 36, 2024.

[9] Yihe Dong, Jean-Baptiste Cordonnier, and Andreas Loukas. Attention is not all you need: Pure attention loses rank doubly exponentially with depth. In *International Conference on Machine Learning*, pages 2793–2803. PMLR, 2021.

[10] Abhimanyu Dubey, Abhinav Jauhri, Abhinav Pandey, Abhishek Kadian, Ahmad Al-Dahle, Aiesha Letman, Akhil Mathur, Alan Schelten, Amy Yang, Angela Fan, et al. The llama 3 herd of models. *arXiv preprint arXiv:2407.21783*, 2024.

[11] Elias Frantar, Saleh Ashkboos, Torsten Hoefler, and Dan Alistarh. Gptq: Accurate post-training quantization for generative pre-trained transformers. *arXiv preprint arXiv:2210.17323*, 2022.

[12] Leo Gao, Jonathan Tow, Baber Abbasi, Stella Biderman, Sid Black, Anthony DiPofi, Charles Foster, Laurence Golding, Jeffrey Hsu, Alain Le Noac'h, Haonan Li, Kyle McDonell, Niklas Muennighoff, Chris Ociepa, Jason Phang, Laria Reynolds, Hailey Schoelkopf, Aviya Skowron, Lintang Sutawika, Eric Tang, Anish Thite, Ben Wang, Kevin Wang, and Andy Zou. A framework for few-shot language model evaluation, 12 2023.

[13] Dan Hendrycks, Collin Burns, Steven Basart, Andy Zou, Mantas Mazeika, Dawn Song, and Jacob Steinhardt. Measuring massive multitask language understanding. In *International Conference on Learning Representations*, 2021.

[14] Jordan Hoffmann, Sebastian Borgeaud, Arthur Mensch, Elena Buchatskaya, Trevor Cai, Eliza Rutherford, Diego de Las Casas, Lisa Anne Hendricks, Johannes Welbl, Aidan Clark, et al. Training compute-optimal large language models. *arXiv preprint arXiv:2203.15556*, 2022.

[15] Coleman Hooper, Sehoon Kim, Hiva Mohammadzadeh, Michael W Mahoney, Yakun Sophia Shao, Kurt Keutzer, and Amir Gholami. Kvquant: Towards 10 million context length llm inference with kv cache quantization. *arXiv preprint arXiv:2401.18079*, 2024.

[16] Minyoung Huh, Hossein Mobahi, Richard Zhang, Brian Cheung, Pulkit Agrawal, and Phillip Isola. The low-rank simplicity bias in deep networks. *arXiv preprint arXiv:2103.10427*, 2021.

[17] Herve Jegou, Matthijs Douze, and Cordelia Schmid. Product quantization for nearest neighbor search. *IEEE transactions on pattern analysis and machine intelligence*, 33(1):117–128, 2010.

[18] Albert Q Jiang, Alexandre Sablayrolles, Arthur Mensch, Chris Bamford, Devendra Singh Chaplot, Diego de las Casas, Florian Bressand, Gianna Lengyel, Guillaume Lample, Lucile Saulnier, et al. Mistral 7b. *arXiv preprint arXiv:2310.06825*, 2023.

[19] Jean Kaddour, Joshua Harris, Maximilian Mozes, Herbie Bradley, Roberta Raileanu, and Robert McHardy. Challenges and applications of large language models. *arXiv preprint arXiv:2307.10169*, 2023.

[20] Sehoon Kim, Coleman Hooper, Amir Gholami, Zhen Dong, Xiuyu Li, Sheng Shen, Michael W Mahoney, and Kurt Keutzer. Squeezellm: Dense-and-sparse quantization. *arXiv preprint arXiv:2306.07629*, 2023.

[21] Alexander Kraskov, Harald Stögbauer, and Peter Grassberger. Estimating mutual information. *Physical review E*, 69(6):066138, 2004.

[22] Yuhang Li, Ruihao Gong, Xu Tan, Yang Yang, Peng Hu, Qi Zhang, Fengwei Yu, Wei Wang, and Shi Gu. Brecq: Pushing the limit of post-training quantization by block reconstruction. *arXiv preprint arXiv:2102.05426*, 2021.

[23] Ji Lin, Jiaming Tang, Haotian Tang, Shang Yang, Xingyu Dang, and Song Han. Awq: Activation-aware weight quantization for llm compression and acceleration. *arXiv preprint arXiv:2306.00978*, 2023.

[24] Zichang Liu, Aditya Desai, Fangshuo Liao, Weitao Wang, Victor Xie, Zhaozhuo Xu, Anastasios Kyrillidis, and Anshumali Shrivastava. Scissorhands: Exploiting the persistence of importance hypothesis for llm kv cache compression at test time. *Advances in Neural Information Processing Systems*, 36, 2024.

[25] Zirui Liu, Jiayi Yuan, Hongye Jin, Shaochen Zhong, Zhaozhuo Xu, Vladimir Braverman, Beidi Chen, and Xia Hu. Kivi: A tuning-free asymmetric 2bit quantization for kv cache. *arXiv preprint arXiv:2402.02750*, 2024.

[26] Stuart Lloyd. Least squares quantization in pcm. *IEEE transactions on information theory*, 28(2):129–137, 1982.

[27] Stephen Merity, Caiming Xiong, James Bradbury, and Richard Socher. Pointer sentinel mixture models. *arXiv preprint arXiv:1609.07843*, 2016.

[28] Amirkeivan Mohtashami and Martin Jaggi. Landmark attention: Random-access infinite context length for transformers. In *Workshop on Efficient Systems for Foundation Models@ ICML2023*.

[29] Adam Paszke, Sam Gross, Francisco Massa, Adam Lerer, James Bradbury, Gregory Chanan, Trevor Killeen, Zeming Lin, Natalia Gimelshein, Luca Antiga, et al. Pytorch: An imperative style, high-performance deep learning library. *Advances in neural information processing systems*, 32, 2019.

[30] Alec Radford, Jeffrey Wu, Rewon Child, David Luan, Dario Amodei, Ilya Sutskever, et al. Language models are unsupervised multitask learners. *OpenAI blog*, 1(8):9, 2019.

[31] Colin Raffel, Noam Shazeer, Adam Roberts, Katherine Lee, Sharan Narang, Michael Matena, Yanqi Zhou, Wei Li, and Peter J Liu. Exploring the limits of transfer learning with a unified text-to-text transformer. *Journal of machine learning research*, 21(140):1–67, 2020.

[32] Keisuke Sakaguchi, Ronan Le Bras, Chandra Bhagavatula, and Yejin Choi. Winogrande: An adversarial winograd schema challenge at scale. *Communications of the ACM*, 64(9):99–106, 2021.

[33] Claude Elwood Shannon. A mathematical theory of communication. *The Bell system technical journal*, 27(3):379–423, 1948.

[34] Ying Sheng, Lianmin Zheng, Binhang Yuan, Zhuohan Li, Max Ryabinin, Beidi Chen, Percy Liang, Christopher Ré, Ion Stoica, and Ce Zhang. Flexgen: High-throughput generative inference of large language models with a single gpu. In *International Conference on Machine Learning*, pages 31094–31116. PMLR, 2023.

[35] Jianlin Su, Murtadha Ahmed, Yu Lu, Shengfeng Pan, Wen Bo, and Yunfeng Liu. Roformer: Enhanced transformer with rotary position embedding. *Neurocomputing*, 568:127063, 2024.

[36] Hugo Touvron, Thibaut Lavril, Gautier Izacard, Xavier Martinet, Marie-Anne Lachaux, Timothée Lacroix, Baptiste Rozière, Naman Goyal, Eric Hambro, Faisal Azhar, et al. Llama: Open and efficient foundation language models. *arXiv preprint arXiv:2302.13971*, 2023.

[37] Hugo Touvron, Louis Martin, Kevin Stone, Peter Albert, Amjad Almahairi, Yasmine Babaei, Nikolay Bashlykov, Soumya Batra, Prajjwal Bhargava, Shruti Bhosale, et al. Llama 2: Open foundation and fine-tuned chat models. *arXiv preprint arXiv:2307.09288*, 2023.

[38] Ashish Vaswani, Noam Shazeer, Niki Parmar, Jakob Uszkoreit, Llion Jones, Aidan N Gomez, Łukasz Kaiser, and Illia Polosukhin. Attention is all you need. *Advances in neural information processing systems*, 30, 2017.

[39] Thomas Wolf, Lysandre Debut, Victor Sanh, Julien Chaumond, Clement Delangue, Anthony Moi, Pierric Cistac, Tim Rault, Rémi Louf, Morgan Funtowicz, et al. Transformers: State-of-the-art natural language processing. In *Proceedings of the 2020 conference on empirical methods in natural language processing: system demonstrations*, pages 38–45, 2020.

[40] Wenhan Xiong, Jingyu Liu, Igor Molybog, Hejia Zhang, Prajjwal Bhargava, Rui Hou, Louis Martin, Rashi Rungta, Karthik Abinav Sankararaman, Barlas Oguz, et al. Effective long-context scaling of foundation models. *arXiv preprint arXiv:2309.16039*, 2023.

[41] Zhichao Xu, Ashim Gupta, Tao Li, Oliver Bentham, and Vivek Srikumar. Beyond perplexity: Multi-dimensional safety evaluation of llm compression. *arXiv preprint arXiv:2407.04965*, 2024.

[42] Rowan Zellers, Ari Holtzman, Yonatan Bisk, Ali Farhadi, and Yejin Choi. Hellaswag: Can a machine really finish your sentence? *arXiv preprint arXiv:1905.07830*, 2019.

[43] Susan Zhang, Stephen Roller, Naman Goyal, Mikel Artetxe, Moya Chen, Shuohui Chen, Christopher Dewan, Mona Diab, Xian Li, Xi Victoria Lin, et al. Opt: Open pre-trained transformer language models. *arXiv preprint arXiv:2205.01068*, 2022.

[44] Tianyi Zhang and Anshumali Shrivastava. Leanquant: Accurate and scalable large language model quantization with loss-error-aware grid. *arXiv preprint arXiv:2407.10032*, 2024.

[45] Tianyi Zhang, Junda Su, Oscar Wu, Zhaozhuo Xu, and Anshumali Shrivastava. Spallm: Unified compressive adaptation of large language models with sketching. *arXiv preprint arXiv:2410.06364*, 2024.

[46] Tianyi Zhang, Jonah Wonkyu Yi, Bowen Yao, Zhaozhuo Xu, and Anshumali Shrivastava. Nomad-attention: Efficient llm inference on cpus through multiply-add-free attention. *arXiv preprint arXiv:2403.01273*, 2024.

[47] Zhenyu Zhang, Ying Sheng, Tianyi Zhou, Tianlong Chen, Lianmin Zheng, Ruisi Cai, Zhao Song, Yuandong Tian, Christopher Ré, Clark Barrett, et al. H2o: Heavy-hitter oracle for efficient generative inference of large language models. *Advances in Neural Information Processing Systems*, 36, 2024.

Appendix / Supplemental Material

A Experimental Details

Perplexity Evaluations Perplexity is evaluated on the test set of the datasets, WikiText-2 and C4, at the maximum context length of the LLMs (2048 for LLaMA, 4096 for LLaMA-2, and 8192 for Mistral), following the setup in [15].

Benchmark Evaluations We use `lm-evaluation-harness` [12] (package version 0.4.2) for performing benchmark evaluations. We use the following task names: `winogrande`, `piqa`, `arc_challenge`, `gsm8k_cot`, `mmlu_flan_cot_fewshot_humanities`, `mmlu_flan_cot_fewshot_stem`, `mmlu_flan_cot_fewshot_social_sciences`, `mmlu_flan_cot_fewshot_other`.

B Perplexity Results on C4

Table 7 presents the perplexity results of different quantization algorithms on the test set of C4 dataset. Our proposed method CQ performs better than or on par with baselines under the same bit width.

Table 7: Perplexity of LLMs on C4 under different KV cache quantization methods at varying bit widths. The results of INT, NF, and KVQuant (except -1b and -1b+1% sparse) are from [15].

Bits Per Activation		LLaMA-7b	LLaMA-13b	LLama-2-7b	LLaMA-2-13b	Mistral-7b
FP16	16	7.08	6.61	6.63	6.05	5.71
INT4	4.00	7.40	6.82	7.31	6.59	5.91
INT4-g128	4.16	7.16	6.67	6.87	6.20	5.76
NF4	4.00	7.27	6.74	7.09	6.45	5.85
NF4-g128	4.25	7.16	6.66	6.86	6.20	5.77
KVQuant-4b	4.00	7.13	6.65	6.70	6.11	5.75
KVQuant-4b+1% sparse	4.32	**7.09**	**6.62**	**6.65**	**6.06**	**5.72**
CQ-2c8b	4.00	7.11	6.64	6.67	6.09	5.74
INT2	2.00	10892	100870	4708	4220	477
INT2-g128	2.14	43.49	56.25	113.49	97.04	50.73
NF2	2.00	2850.1	4680.3	13081.2	4175.6	1102.3
NF2-g128	2.25	248.32	118.18	420.05	499.82	191.73
KVQuant-2b	2.00	10.28	9.05	15.16	43.77	8.40
KVQuant-2b+1% sparse	2.32	7.38	**6.83**	7.06	6.38	6.08
CQ-4c8b	2.00	7.52	6.96	7.23	6.52	6.17
CQ-4c9b	2.26	**7.37**	6.84	**7.02**	**6.36**	**5.99**
KVQuant-1b	1.00	168.90	1316.41	362.94	4223.37	127.07
KVQuant-1b+1% sparse	1.32	11.18	9.56	16.04	22.87	10.53
CQ-8c8b	1.00	12.13	10.53	12.49	10.53	9.89
CQ-8c10b	1.27	**9.12**	**8.23**	**9.03**	**8.01**	**7.46**

C Effects of Channel-coupling and Fisher-guided Centroid Learning

We validate the effectiveness of our proposed channel-coupling and Fisher-guided centroid learning by compressing LLaMA-7b KV cache to 1-bit and 2-bit, and present the perplexity results and quantization errors ($\|A - \mathrm{cq}(A)\|_F^2$ averaged over layers) on WikiText-2 under different CQ configurations in Figure 5. As the number of coupled channels increases, perplexity improves significantly and approaches the FP16 performance. The quantization errors of keys and values also decrease as the number of coupled channels increase. Although Fisher-guided centroid learning increases the quantization error, it better preserves the salient activations and achieves lower perplexity.

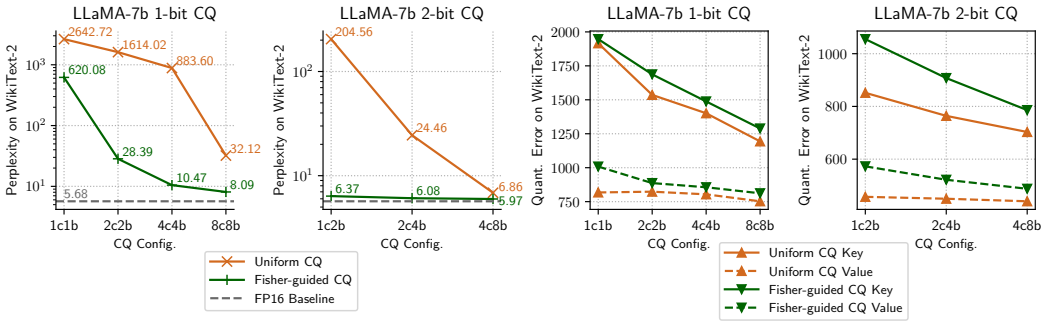

Figure 5: Perplexity and key/value quantization errors (averaged over all layers) of LLaMA-7b on WikiText-2. Channels coupling and Fisher-guided centroid learning are effective for improving perplexity.

D Ablation Study on More Models

We study the effectiveness of each component of our proposed approach in Table 8. We evaluate the perplexity of 2 models Mistral-7b and LLaMA-2-13b on WikiText-2 using CQ at 2 bits per activation, with varying number of channels coupled and comparing uniform centroid learning and Fisher-guided centroid learning. Fisher-guided centroids significantly improve model quality as demonstrated by lower perplexity. With either uniform centroids or Fisher-guided centroids, perplexity improves as the number of coupled channels increases. Hence, our proposed techniques of channel coupling and Fisher-guided centroid learning are both effective for maintaining model quality.

Table 8: Perplexity of different models on WikiText-2 using CQ with varying number of coupled channels and fisher-guided centroids. Perplexity consistently improves as the number of coupled channels increases.

	Mistral-7b						LLaMA-2-13b					
Bits Per Activation	2	2	2	2	2	2	2	2	2	2	2	2
Num. of Channels Coupled	1	2	4	1	2	4	1	2	4	1	2	4
Fisher-guided Centroids	✗	✗	✗	✓	✓	✓	✗	✗	✗	✓	✓	✓
Perplexity ↓	97.76	16.29	5.42	5.34	5.20	5.11	890.42	171.96	6.62	6.06	4.91	4.81

E Overhead of Centroid Learning and Storage

We present the computational overhead of centroid learning and the memory overhead of centroid storage for CQ in Table 9. The centroid learning process of CQ consists of many independent k-means runs, which can be time-consuming on CPUs. Hence, we leverage a GPU implementation to accelerate the learning process. In all our experiments, we use k-means++ initialization and run 100 iterations of k-means on a single GPU to obtain the centroids. The memory overhead of storing the centroids can be calculated as $l \times 2 \times h \times d \times 2^b$ FP16 numbers, where l is the number of layers, 2 is for keys and values, h is the number of key/value attention heads, d is the number of channels in a single-head key/value activation embedding, and b is the bit width of quantized codes. As shown in Table 9, CQ can easily scale to large model sizes with low learning and memory overheads.

F Bits Per Activation Calculations for CQ

To calculate bits per activation, we assume the batch size is 16 and the sequence length is 65,536. For CQ-ccbb, the storage of quantized codes requires the following number of bits

$$16 \times 65536 \times l \times 2 \times h \times d \times b/c$$

where l is the number of layers, 2 is for key and value, h is the number of key/value attention heads, d is the number of channels for a single head of attention, and b/c is the average number of bits per token per channel.

Table 9: Learning and memory overhead of different CQ configurations and models. The number of centroid parameters are shown in millions, and the percentage to the model weights is shown in brackets.

	Centroid Learning Time					Parameter Count in Centroids				
CQ Config.	2c8b	4c8b	4c9b	8c8b	8c10b	2c8b	4c8b	4c9b	8c8b	8c10b
LLaMA-7b	53 mins	28 mins	62 mins	14 mins	104 mins	67.11M (0.996%)	67.11M (0.996%)	134.22M (1.992%)	67.11M (0.996%)	268.44M (3.984%)
LLaMA-13b	94 mins	44 mins	96 mins	22 mins	160 mins	104.86M (0.806%)	104.86M (0.806%)	209.72M (1.612%)	104.86M (0.806%)	419.43M (3.224%)
LLaMA-2-7b	54 mins	28 mins	62 mins	14 mins	104 mins	67.11M (0.996%)	67.11M (0.996%)	134.22M (1.992%)	67.11M (0.996%)	268.44M (3.984%)
LLaMA-2-13b	83 mins	44 mins	96 mins	23 mins	162 mins	104.86M (0.806%)	104.86M (0.806%)	209.72M (1.612%)	104.86M (0.806%)	419.43M (3.224%)
Mistral-7b	13 mins	7 mins	15 mins	4 mins	27 mins	16.78M (0.232%)	16.78M (0.232%)	33.56M (0.464%)	16.78M (0.232%)	67.11M (0.928%)

The learned centroids of CQ are stored in FP16 format. Hence the storage of CQ centroids requires the following number of bits

$$l \times 2 \times h \times d \times 2^b \times 16$$

CQ has no other storage overhead besides quantized codes and centroids. Therefore, the average bits per activation for CQ-ccbb is calculated as

$$\begin{aligned}&\frac{16 \times 65536 \times l \times 2 \times h \times d \times b/c + l \times 2 \times h \times d \times 2^b \times 16}{16 \times 65536 \times l \times 2 \times h \times d \times 16} \times 16 \\ =&\frac{65536 \times b/c + 2^b}{65536}\end{aligned}$$

G Generalizability of Learned Centroids

Centroids for CQ are learned once on a calibration dataset and can be used for different downstream tasks. We perform an ablation study to examine the effects of calibration data on the quality of learned CQ centroids. We use 16 sequences of 2048 tokens from different datasets as the calibration set for CQ and evaluate on 4 downstream tasks, and the results are presented in Table 10. Despite using different calibration datasets, CQ performs similarly in various downstream tasks. The results suggest that calibration on language modeling datasets, such as WikiText-2 and C4, provides transferable performance on downstream tasks.

Table 10: Zero-shot accuracy of LLaMA-2-7b with couple-quantized KV cache, calibrated using two different datasets WikiText-2 and C4. CQ displays similar accuracy in various downstream tasks, despite using different calibration datasets.

		Downstream Task			
	Calibration Dataset	WinoGrande	PIQA	Arc-C	GSM8K CoT
CQ-2c8b	WikiText-2	68.27	77.91	43.34	14.71
	C4	68.35	77.86	43.16	14.71
CQ-4c8b	WikiText-2	66.45	76.12	39.93	8.04
	C4	66.22	76.61	39.93	8.34
CQ-8c8b	WikiText-2	55.01	71.22	30.20	1.74
	C4	56.27	71.55	30.52	1.90

Table 11: Accuracy comparison of CQ and KIVI on LongBench for LLaMA-2-7b. The results of KIVI are from [25].

	Sliding Window Size	Qasper	QMSum	MultiNews	TREC	TriviaQA	SAMSum	LCC	RepoBench-P
FP16	-	9.52	21.28	3.51	66.00	87.72	41.69	66.66	59.82
KIVI-2b	32	9.26	20.53	0.97	**66.00**	87.42	**42.61**	66.22	59.67
CQ-4c8b	32	**9.58**	**20.87**	**1.93**	**66.00**	**87.72**	41.13	**66.57**	**59.75**

H Comparison with KIVI

We perform an empirical comparison of CQ with KIVI [25] using LLaMA-2-7b on LongBench [2]. For both methods, we use 2-bit quantization and a sliding-window full-precision cache of 32 tokens. We compare CQ-4c8b against KIVI with a group size of 32. The accuracy results are presented in Table 11. CQ mostly outperforms KIVI in preserving model accuracy.

I Passkey Retrieval

We compare the quantization quality of CQ and KVQuant by evaluating them on the passkey retrieval task [28]. We follow the setup in [15], and measure the success rate of passkey retrieval for LLaMA-2-7b at its maximum context length of 4096. Table 12 presents the passkey retrieval results, where CQ outperforms or performs the same as KVQuant at various bit widths.

Table 12: The passkey retrieval success rate of CQ and KVQuant at different quantization bit widths, for LLaMA-2-7b at its maximum context length of 4096.

	Bit Width	Success Rate
KVQuant-4b+1% sparse	4.32	**100%**
KVQuant-4b	4.00	**100%**
CQ-2c8b	4.00	**100%**
KVQuant-2b+1% sparse	2.32	94%
CQ-4c9b	2.26	**98%**
KVQuant-2b	2.00	0%
CQ-4c8b	2.00	**96%**
KVQuant-1b+1% sparse	1.32	2%
CQ-8c10b	1.27	**78%**
KVQuant-1b	1.00	0%
CQ-8c8b	1.00	**12%**

J Results on LLaMA 3

We evaluate the effectiveness of CQ and KVQuant for quantizing the KV cache of the LLaMA 3 model [10]. For both methods, we quantize the KV cache of all tokens of the LLaMA-3-8b model, and perform the calibration on 16 sequences from the training set of WikiText-2 and evaluate perplexity on the test set, and benchmark on 3 downstream tasks: WinoGrande, PIQA and Arc Challenge. The results are presented in Table [10]. CQ mostly outperforms KVQuant, especially in lower bit widths.

Table 13: The effectiveness of CQ and KVQuant on LLaMA-3-8b.

	Bits Per Activation	WikiText-2 PPL ↓	WinoGrande ↑	PIQA ↑	Arc-C ↑
FP16	16	5.54	72.69	79.71	50.51
KVQuant-4b	4.00	5.66	72.77	**79.98**	47.44
CQ-2c8b	4.00	**5.58**	**73.16**	78.84	**49.83**
KVQuant-2b	2.00	18.96	56.27	63.49	24.40
CQ-4c8b	2.00	**6.09**	**69.22**	**78.62**	**44.03**
KVQuant-1b	1.00	22238.91	50.04	53.05	22.35
CQ-8c8b	1.00	**9.56**	**56.04**	**72.58**	**32.51**

K Latency Measurements

We measure the prefill and decoding latency of CQ, with and without a sliding window of full-precision cache, and compare against KIVI [25] and full-precision FP16 cache. The latency mea-

surements are conducted on a single A100-40GB GPU for LLaMA-2-7b with a batch size of 1 and a prompt length of 2000 tokens The results are presented in Table 14. CQ achieves prefill and decoding latency on par with KIVI.

Table 14: Latency measurements of decoding LLaMA-2-7b with a batch size of 1 and a prompt of 2000 tokens, averaged over 100 tokens, using FP16 KV cache, and CQ and KIVI quantized KV cache.

	Full-precision Sliding-window Length	Prefill Time (s)	Decoding Time (s)
FP16	-	0.853	0.0559 ± 0.0044
KIVI-4b	32	1.483	0.0693 ± 0.0212
KIVI-2b	32	1.291	0.0684 ± 0.0213
CQ-2c8b	0	1.820	0.0695 ± 0.0056
CQ-2c8b	32	1.926	0.0701 ± 0.0057
CQ-4c8b	0	1.684	0.0704 ± 0.0056
CQ-4c8b	32	1.790	0.0706 ± 0.0058
CQ-8c8b	0	1.726	0.0670 ± 0.0070
CQ-8c8b	32	1.857	0.0799 ± 0.0066

L Extreme Sub-1-bit Quantization

We demonstrate the effectiveness of CQ by performing extreme sub-1-bit quantization with LLaMA-7b. We evaluate the perplexity of CQ-16c12b, which use a 12-bit code for every group of 16 coupled channels, averaging 0.81 bits per activation. Table 15 presents the results with comparison to FP16 cache and KVQuant-1b. CQ preserves model quality reasonably under extreme KV cache compression.

Table 15: Perplexity of LLaMA-7b under extreme KV cache compression with CQ-16c12b (12 bits per 16 coupled channels, averaging 0.81 bits per activation).

	BPA	WikiText-2 ↓	C4 ↓
FP16	16	5.68	7.08
KVQuant-1b	1.00	321.58	168.90
CQ-16c12b	0.81	8.71	14.40

M Correlation Matrices and Scatter Plots

Figure 6 and 7 show the correlation matrices for key and value channels of each layer of the LLaMA-7b model on 262k tokens of WikiText-2. Figure 8 and 9 present the 2D scatter plots of key and value channel pairs of 4 layers of the LLaMA-7b model on 262k tokens of WikiText-2.

N Variations in Channel Correlation

As shown in Figure 6 and 7, the amount of correlation between channels varies depending on the layer. In Table 16, we study this variation by presenting the mean absolute correlation (MAC), excluding the diagonals, for different layers of LLaMA-7b on 262K tokens of WikiText-2. Although the key correlation of the first few layers are significantly higher than the later layers, the key/value correlation of any layer is never very close to zero, meaning channel coupling can be effective for any layer. Furthermore, the ablation study presented in Table 5 also demonstrates the effectivenss of channel coupling for capturing the channel correlation.

O Limitations

Low-bit quantization is a type of lossy model compression, which affects the model quality including metrics such as perplexity and accuracy, and also impacts model safety including toxicity and bias [41]. This work does not study the effects of extreme low-bit quantization of KV cache on the safety aspects of the model.

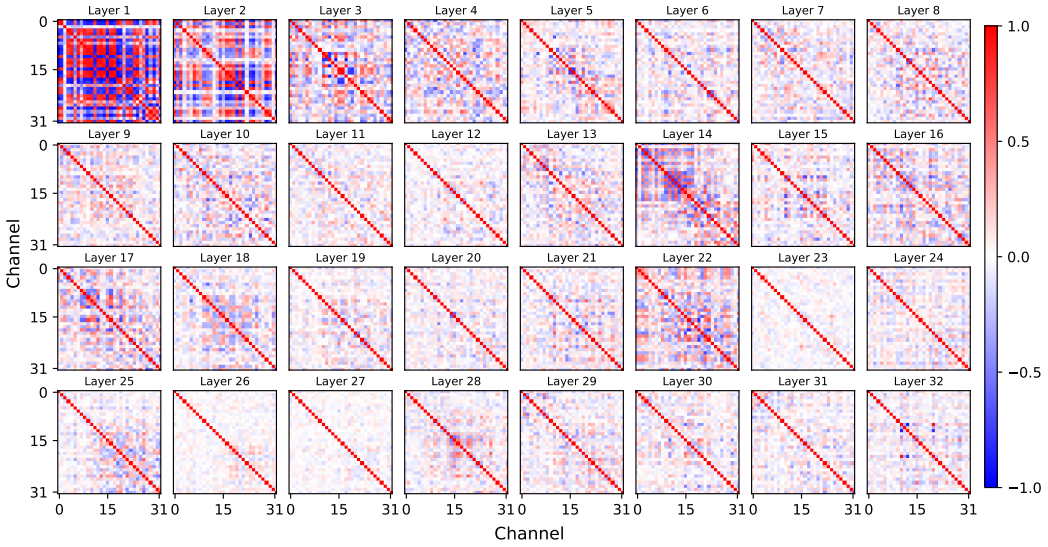

Figure 6: Correlation matrix for the first 32 channels of pre-RoPE **key** activation embeddings of all LLaMA-7b layers on WikiText-2.

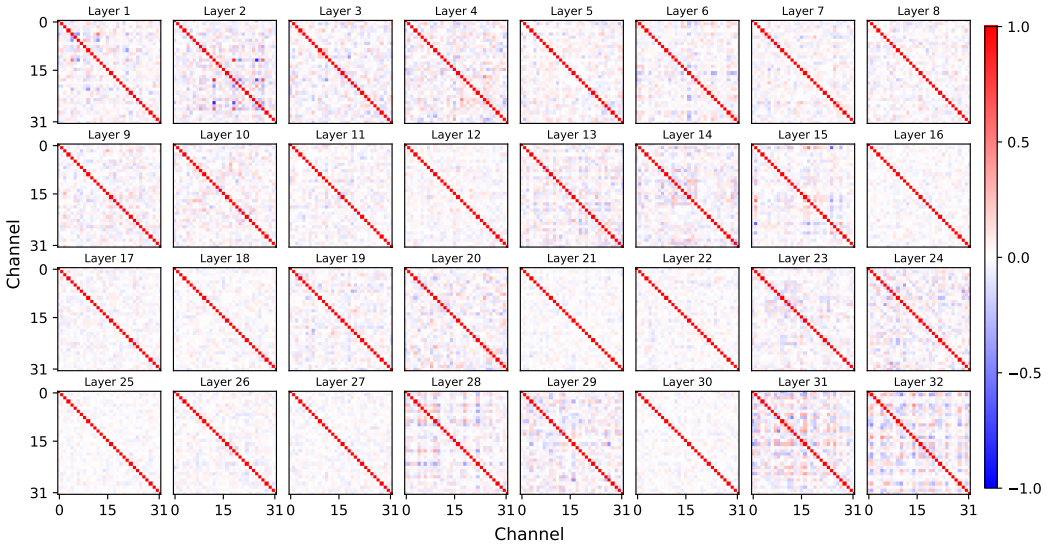

Figure 7: Correlation matrix for the first 32 channels of **value** activation embeddings of all LLaMA-7b layers on WikiText-2.

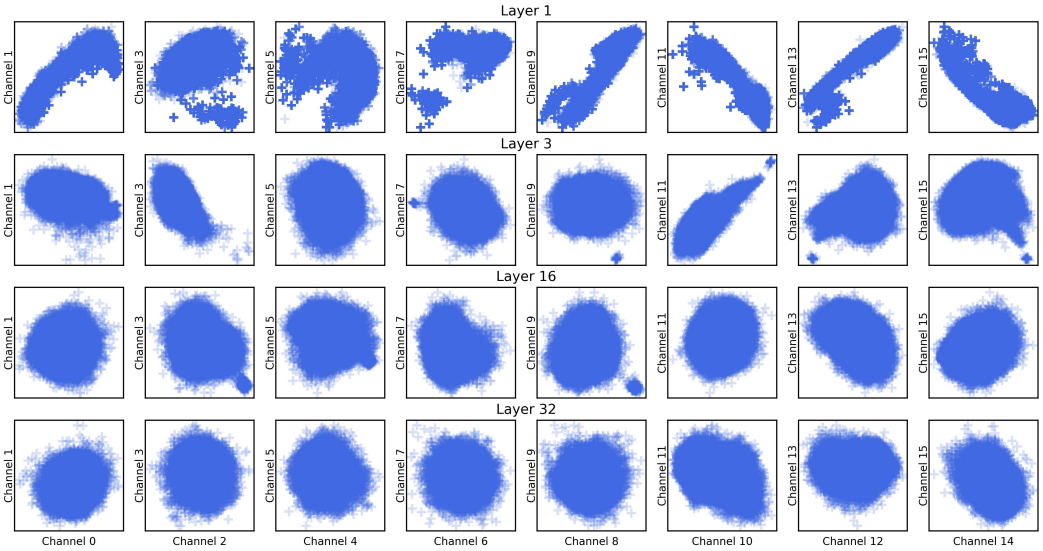

Figure 8: Scatter plots of pairs of channels in pre-RoPE **key** activation embeddings of 4 LLaMA-7b layers on WikiText-2.

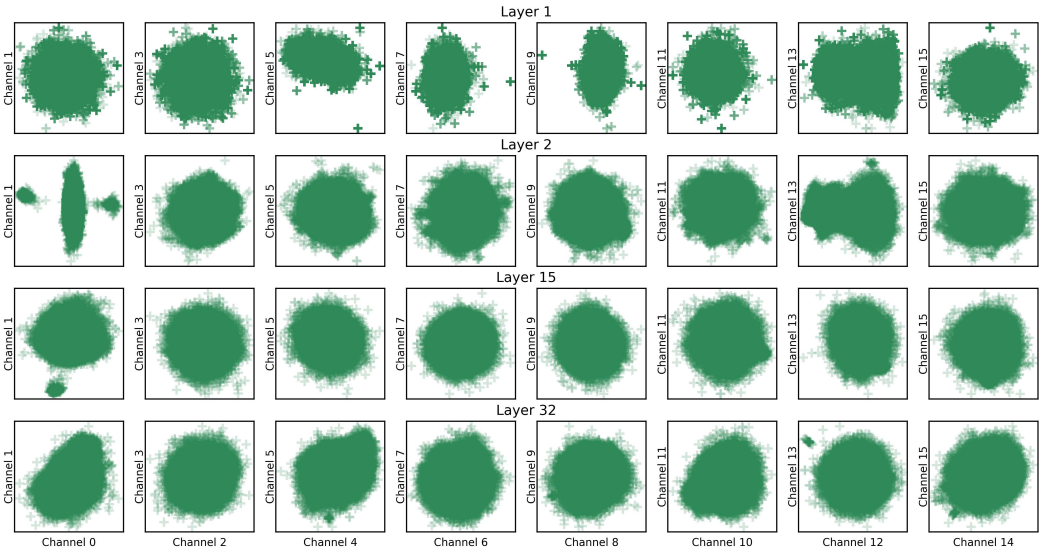

Figure 9: Scatter plots of pairs of channels in **value** activation embeddings of 4 LLaMA-7b layers on WikiText-2.

Table 16: The mean absolute correlation (MAC), excluding the diagonals, of key/value channels in different layers of LLaMA-7b, computed on 262K tokens of WikiText-2.

Layer	1	2	3	4	5	6	7	8
Key	0.407	0.212	0.193	0.178	0.114	0.113	0.115	0.122
Value	0.071	0.084	0.061	0.073	0.055	0.056	0.056	0.057
Layer	9	10	11	12	13	14	15	16
Key	0.131	0.138	0.090	0.098	0.094	0.141	0.109	0.114
Value	0.061	0.067	0.047	0.042	0.065	0.065	0.062	0.035
Layer	17	18	19	20	21	22	23	24
Key	0.136	0.111	0.091	0.101	0.102	0.156	0.071	0.094
Value	0.039	0.038	0.052	0.070	0.031	0.038	0.061	0.074
Layer	25	26	27	28	29	30	31	32
Key	0.107	0.069	0.057	0.103	0.095	0.097	0.100	0.090
Value	0.027	0.044	0.038	0.072	0.070	0.035	0.105	0.090

NeurIPS Paper Checklist

1. **Claims**

   Question: Do the main claims made in the abstract and introduction accurately reflect the paper's contributions and scope?

   Answer: [Yes]

   Justification: All of our claims made in the abstract and the introduction are supported by the results presented in "Experiments" section, and they accurately reflect the paper's contributions and scope as shown in the "Background" and "Methodology" sections.

   Guidelines:

   - The answer NA means that the abstract and introduction do not include the claims made in the paper.
   - The abstract and/or introduction should clearly state the claims made, including the contributions made in the paper and important assumptions and limitations. A No or NA answer to this question will not be perceived well by the reviewers.
   - The claims made should match theoretical and experimental results, and reflect how much the results can be expected to generalize to other settings.
   - It is fine to include aspirational goals as motivation as long as it is clear that these goals are not attained by the paper.

2. **Limitations**

   Question: Does the paper discuss the limitations of the work performed by the authors?

   Answer: [Yes]

   Justification: We have made clear the limitations of our proposal, and included a separate "Limitations & Broader Impacts" section.

   Guidelines:

   - The answer NA means that the paper has no limitation while the answer No means that the paper has limitations, but those are not discussed in the paper.
   - The authors are encouraged to create a separate "Limitations" section in their paper.
   - The paper should point out any strong assumptions and how robust the results are to violations of these assumptions (e.g., independence assumptions, noiseless settings, model well-specification, asymptotic approximations only holding locally). The authors should reflect on how these assumptions might be violated in practice and what the implications would be.
   - The authors should reflect on the scope of the claims made, e.g., if the approach was only tested on a few datasets or with a few runs. In general, empirical results often depend on implicit assumptions, which should be articulated.
   - The authors should reflect on the factors that influence the performance of the approach. For example, a facial recognition algorithm may perform poorly when image resolution is low or images are taken in low lighting. Or a speech-to-text system might not be used reliably to provide closed captions for online lectures because it fails to handle technical jargon.
   - The authors should discuss the computational efficiency of the proposed algorithms and how they scale with dataset size.
   - If applicable, the authors should discuss possible limitations of their approach to address problems of privacy and fairness.
   - While the authors might fear that complete honesty about limitations might be used by reviewers as grounds for rejection, a worse outcome might be that reviewers discover limitations that aren't acknowledged in the paper. The authors should use their best judgment and recognize that individual actions in favor of transparency play an important role in developing norms that preserve the integrity of the community. Reviewers will be specifically instructed to not penalize honesty concerning limitations.

3. **Theory Assumptions and Proofs**

   Question: For each theoretical result, does the paper provide the full set of assumptions and a complete (and correct) proof?

Answer: [NA]

Justification: We present no new theoretical results in this paper.

Guidelines:

- The answer NA means that the paper does not include theoretical results.
- All the theorems, formulas, and proofs in the paper should be numbered and cross-referenced.
- All assumptions should be clearly stated or referenced in the statement of any theorems.
- The proofs can either appear in the main paper or the supplemental material, but if they appear in the supplemental material, the authors are encouraged to provide a short proof sketch to provide intuition.
- Inversely, any informal proof provided in the core of the paper should be complemented by formal proofs provided in appendix or supplemental material.
- Theorems and Lemmas that the proof relies upon should be properly referenced.

4. **Experimental Result Reproducibility**

   Question: Does the paper fully disclose all the information needed to reproduce the main experimental results of the paper to the extent that it affects the main claims and/or conclusions of the paper (regardless of whether the code and data are provided or not)?

   Answer: [Yes]

   Justification: The paper fully discloses all information for reproducing the experimental results, including algorithmic details, parameters, experimental setup, and baselines in the "Methodology" and "Experiments" sections.

   Guidelines:

   - The answer NA means that the paper does not include experiments.
   - If the paper includes experiments, a No answer to this question will not be perceived well by the reviewers: Making the paper reproducible is important, regardless of whether the code and data are provided or not.
   - If the contribution is a dataset and/or model, the authors should describe the steps taken to make their results reproducible or verifiable.
   - Depending on the contribution, reproducibility can be accomplished in various ways. For example, if the contribution is a novel architecture, describing the architecture fully might suffice, or if the contribution is a specific model and empirical evaluation, it may be necessary to either make it possible for others to replicate the model with the same dataset, or provide access to the model. In general. releasing code and data is often one good way to accomplish this, but reproducibility can also be provided via detailed instructions for how to replicate the results, access to a hosted model (e.g., in the case of a large language model), releasing of a model checkpoint, or other means that are appropriate to the research performed.
   - While NeurIPS does not require releasing code, the conference does require all submissions to provide some reasonable avenue for reproducibility, which may depend on the nature of the contribution. For example
     (a) If the contribution is primarily a new algorithm, the paper should make it clear how to reproduce that algorithm.
     (b) If the contribution is primarily a new model architecture, the paper should describe the architecture clearly and fully.
     (c) If the contribution is a new model (e.g., a large language model), then there should either be a way to access this model for reproducing the results or a way to reproduce the model (e.g., with an open-source dataset or instructions for how to construct the dataset).
     (d) We recognize that reproducibility may be tricky in some cases, in which case authors are welcome to describe the particular way they provide for reproducibility. In the case of closed-source models, it may be that access to the model is limited in some way (e.g., to registered users), but it should be possible for other researchers to have some path to reproducing or verifying the results.

5. **Open access to data and code**

Question: Does the paper provide open access to the data and code, with sufficient instructions to faithfully reproduce the main experimental results, as described in supplemental material?

Answer: [No]

Justification: The code is proprietary to xMAD.ai. However, anyone is able to reproduce our results using the algorithm and procedure we describe in the paper. We will provide a mechanism to reproduce our numbers in the future.

Guidelines:

- The answer NA means that paper does not include experiments requiring code.
- Please see the NeurIPS code and data submission guidelines (`https://nips.cc/public/guides/CodeSubmissionPolicy`) for more details.
- While we encourage the release of code and data, we understand that this might not be possible, so "No" is an acceptable answer. Papers cannot be rejected simply for not including code, unless this is central to the contribution (e.g., for a new open-source benchmark).
- The instructions should contain the exact command and environment needed to run to reproduce the results. See the NeurIPS code and data submission guidelines (`https://nips.cc/public/guides/CodeSubmissionPolicy`) for more details.
- The authors should provide instructions on data access and preparation, including how to access the raw data, preprocessed data, intermediate data, and generated data, etc.
- The authors should provide scripts to reproduce all experimental results for the new proposed method and baselines. If only a subset of experiments are reproducible, they should state which ones are omitted from the script and why.
- At submission time, to preserve anonymity, the authors should release anonymized versions (if applicable).
- Providing as much information as possible in supplemental material (appended to the paper) is recommended, but including URLs to data and code is permitted.

6. **Experimental Setting/Details**

Question: Does the paper specify all the training and test details (e.g., data splits, hyperparameters, how they were chosen, type of optimizer, etc.) necessary to understand the results?

Answer: [Yes]

Justification: We specify all relevant experimental details in the paper for understanding the results in the "Experiments" section.

Guidelines:

- The answer NA means that the paper does not include experiments.
- The experimental setting should be presented in the core of the paper to a level of detail that is necessary to appreciate the results and make sense of them.
- The full details can be provided either with the code, in appendix, or as supplemental material.

7. **Experiment Statistical Significance**

Question: Does the paper report error bars suitably and correctly defined or other appropriate information about the statistical significance of the experiments?

Answer: [Yes]

Justification: We report error bars where applicable.

Guidelines:

- The answer NA means that the paper does not include experiments.
- The authors should answer "Yes" if the results are accompanied by error bars, confidence intervals, or statistical significance tests, at least for the experiments that support the main claims of the paper.

- The factors of variability that the error bars are capturing should be clearly stated (for example, train/test split, initialization, random drawing of some parameter, or overall run with given experimental conditions).
- The method for calculating the error bars should be explained (closed form formula, call to a library function, bootstrap, etc.)
- The assumptions made should be given (e.g., Normally distributed errors).
- It should be clear whether the error bar is the standard deviation or the standard error of the mean.
- It is OK to report 1-sigma error bars, but one should state it. The authors should preferably report a 2-sigma error bar than state that they have a 96% CI, if the hypothesis of Normality of errors is not verified.
- For asymmetric distributions, the authors should be careful not to show in tables or figures symmetric error bars that would yield results that are out of range (e.g. negative error rates).
- If error bars are reported in tables or plots, The authors should explain in the text how they were calculated and reference the corresponding figures or tables in the text.

8. **Experiments Compute Resources**

   Question: For each experiment, does the paper provide sufficient information on the computer resources (type of compute workers, memory, time of execution) needed to reproduce the experiments?

   Answer: [Yes]

   Justification: We provide detailed information on the resources needed for reproducing the experiments in the "Experiments" section.

   Guidelines:

   - The answer NA means that the paper does not include experiments.
   - The paper should indicate the type of compute workers CPU or GPU, internal cluster, or cloud provider, including relevant memory and storage.
   - The paper should provide the amount of compute required for each of the individual experimental runs as well as estimate the total compute.
   - The paper should disclose whether the full research project required more compute than the experiments reported in the paper (e.g., preliminary or failed experiments that didn't make it into the paper).

9. **Code Of Ethics**

   Question: Does the research conducted in the paper conform, in every respect, with the NeurIPS Code of Ethics `https://neurips.cc/public/EthicsGuidelines`?

   Answer: [Yes]

   Justification: We have reviewed the NeurIPS Code of Ethics and can confirm that our paper conforms with it in every respect.

   Guidelines:

   - The answer NA means that the authors have not reviewed the NeurIPS Code of Ethics.
   - If the authors answer No, they should explain the special circumstances that require a deviation from the Code of Ethics.
   - The authors should make sure to preserve anonymity (e.g., if there is a special consideration due to laws or regulations in their jurisdiction).

10. **Broader Impacts**

    Question: Does the paper discuss both potential positive societal impacts and negative societal impacts of the work performed?

    Answer: [Yes]

    Justification: We include an "Limitations & Broader Impacts" section to discuss our potential societal impacts.

    Guidelines:

- The answer NA means that there is no societal impact of the work performed.
- If the authors answer NA or No, they should explain why their work has no societal impact or why the paper does not address societal impact.
- Examples of negative societal impacts include potential malicious or unintended uses (e.g., disinformation, generating fake profiles, surveillance), fairness considerations (e.g., deployment of technologies that could make decisions that unfairly impact specific groups), privacy considerations, and security considerations.
- The conference expects that many papers will be foundational research and not tied to particular applications, let alone deployments. However, if there is a direct path to any negative applications, the authors should point it out. For example, it is legitimate to point out that an improvement in the quality of generative models could be used to generate deepfakes for disinformation. On the other hand, it is not needed to point out that a generic algorithm for optimizing neural networks could enable people to train models that generate Deepfakes faster.
- The authors should consider possible harms that could arise when the technology is being used as intended and functioning correctly, harms that could arise when the technology is being used as intended but gives incorrect results, and harms following from (intentional or unintentional) misuse of the technology.
- If there are negative societal impacts, the authors could also discuss possible mitigation strategies (e.g., gated release of models, providing defenses in addition to attacks, mechanisms for monitoring misuse, mechanisms to monitor how a system learns from feedback over time, improving the efficiency and accessibility of ML).

11. **Safeguards**

    Question: Does the paper describe safeguards that have been put in place for responsible release of data or models that have a high risk for misuse (e.g., pretrained language models, image generators, or scraped datasets)?

    Answer: [NA]

    Justification: We release no new models or datasets.

    Guidelines:

    - The answer NA means that the paper poses no such risks.
    - Released models that have a high risk for misuse or dual-use should be released with necessary safeguards to allow for controlled use of the model, for example by requiring that users adhere to usage guidelines or restrictions to access the model or implementing safety filters.
    - Datasets that have been scraped from the Internet could pose safety risks. The authors should describe how they avoided releasing unsafe images.
    - We recognize that providing effective safeguards is challenging, and many papers do not require this, but we encourage authors to take this into account and make a best faith effort.

12. **Licenses for existing assets**

    Question: Are the creators or original owners of assets (e.g., code, data, models), used in the paper, properly credited and are the license and terms of use explicitly mentioned and properly respected?

    Answer: [Yes]

    Justification: We properly credit and respect the licenses and terms of the assets we use in our work.

    Guidelines:

    - The answer NA means that the paper does not use existing assets.
    - The authors should cite the original paper that produced the code package or dataset.
    - The authors should state which version of the asset is used and, if possible, include a URL.
    - The name of the license (e.g., CC-BY 4.0) should be included for each asset.

- For scraped data from a particular source (e.g., website), the copyright and terms of service of that source should be provided.
- If assets are released, the license, copyright information, and terms of use in the package should be provided. For popular datasets, `paperswithcode.com/datasets` has curated licenses for some datasets. Their licensing guide can help determine the license of a dataset.
- For existing datasets that are re-packaged, both the original license and the license of the derived asset (if it has changed) should be provided.
- If this information is not available online, the authors are encouraged to reach out to the asset's creators.

13. **New Assets**

    Question: Are new assets introduced in the paper well documented and is the documentation provided alongside the assets?

    Answer: [Yes]

    Justification: New assets are documented where applicable.

    Guidelines:

    - The answer NA means that the paper does not release new assets.
    - Researchers should communicate the details of the dataset/code/model as part of their submissions via structured templates. This includes details about training, license, limitations, etc.
    - The paper should discuss whether and how consent was obtained from people whose asset is used.
    - At submission time, remember to anonymize your assets (if applicable). You can either create an anonymized URL or include an anonymized zip file.

14. **Crowdsourcing and Research with Human Subjects**

    Question: For crowdsourcing experiments and research with human subjects, does the paper include the full text of instructions given to participants and screenshots, if applicable, as well as details about compensation (if any)?

    Answer: [NA]

    Justification: Our paper does not involve crowdsourcing or research with human subjects.

    Guidelines:

    - The answer NA means that the paper does not involve crowdsourcing nor research with human subjects.
    - Including this information in the supplemental material is fine, but if the main contribution of the paper involves human subjects, then as much detail as possible should be included in the main paper.
    - According to the NeurIPS Code of Ethics, workers involved in data collection, curation, or other labor should be paid at least the minimum wage in the country of the data collector.

15. **Institutional Review Board (IRB) Approvals or Equivalent for Research with Human Subjects**

    Question: Does the paper describe potential risks incurred by study participants, whether such risks were disclosed to the subjects, and whether Institutional Review Board (IRB) approvals (or an equivalent approval/review based on the requirements of your country or institution) were obtained?

    Answer: [NA]

    Justification: Our paper does not involve crowdsourcing or research with human subjects.

    Guidelines:

    - The answer NA means that the paper does not involve crowdsourcing nor research with human subjects.

- Depending on the country in which research is conducted, IRB approval (or equivalent) may be required for any human subjects research. If you obtained IRB approval, you should clearly state this in the paper.
- We recognize that the procedures for this may vary significantly between institutions and locations, and we expect authors to adhere to the NeurIPS Code of Ethics and the guidelines for their institution.
- For initial submissions, do not include any information that would break anonymity (if applicable), such as the institution conducting the review.